© 2016. Published by The Company of Biologists Ltd | Journal of Cell Science (2016) 129, 557-568 doi:10.1242/jcs.179374

RESEARCH ARTICLE

Cathepsin D and its newly identified transport receptor SEZ6L2 can modulate neurite outgrowth

Marielle Boonen[1], Catherine Staudt[1], Florentine Gilis[1], Viola Oorschot[2], Judith Klumperman[2] and Michel Jadot[1,*]

ABSTRACT

How, in the absence of a functional mannose 6-phosphate (Man-6-P)-signal-dependent transport pathway, some acid hydrolases remain sorted to endolysosomes in the brain is poorly understood. We demonstrate that cathepsin D binds to mouse SEZ6L2, a type 1 transmembrane protein predominantly expressed in the brain. Studies of the subcellular trafficking of SEZ6L2, and its silencing in a mouse neuroblastoma cell line reveal that SEZ6L2 is involved in the trafficking of cathepsin D to endosomes. Moreover, SEZ6L2 can partially correct the cathepsin D hypersecretion resulting from the knockdown of UDP-GlcNAc:lysosomal enzyme GlcNAc-1-phosphotransferase in HeLa cells (i.e. in cells that are unable to synthesize Man-6-P signals). Interestingly, cleavage of SEZ6L2 by cathepsin D generates an N-terminal soluble fragment that induces neurite outgrowth, whereas its membrane counterpart prevents this. Taken together, our findings highlight that SEZ6L2 can serve as receptor to mediate the sorting of cathepsin D to endosomes, and suggest that proteolytic cleavage of SEZ6L2 by cathepsin D modulates neuronal differentiation.

KEY WORDS: Lysosomal hydrolase, Transport receptor, Mannose 6-phosphate-independent

INTRODUCTION

Most lysosomal hydrolases are targeted to endolysosomes from the trans-Golgi network (TGN) using the mannose 6-phosphate (Man-6-P)-dependent pathway. In this pathway, Man-6-P moieties added onto their high-mannose glycans in the Golgi are recognized by Man-6-P receptors (MPRs), which initiate the hydrolase packaging into clathrin-coated vesicles that travel to pre-lysosomal compartments (Ghosh et al., 2003; Braulke and Bonifacino, 2009). Acid hydrolase can also reach endolysosomes after endocytosis by the cation-independent MPR. In the absence of UDP-GlcNAc:lysosomal enzyme GlcNAc-1-phosphotransferase (also known as GlcNAc-1-phosphotransferase; hereafter Ptase) (the first enzyme involved in Man-6-P synthesis), or upon knockdown of MPRs, fibroblasts and other cells of mesenchymal origin, as well as acinar secretory cells, missort their acid hydrolases, causing lysosomal dysfunction (Ludwig et al., 1994; Pohlmann et al., 1995; Kornfeld and Sly, 2000; Boonen et al., 2011). However, intriguingly, the aspartic protease cathespin D can still reach lysosomes in several cell types (Rijnboutt et al., 1991; Glickman and Kornfeld, 1993; Dittmer et al., 1999; Pohl et al., 2010; van Meel et al., 2011; Markmann et al., 2015). Moreover, previous work showed that the intracellular level and processing of cathepsin D (indicative of its lysosomal sorting) is close to normal in the brain of Ptase-deficient (Boonen et al., 2011, our unpublished data) or Ptase knock-in (Kollmann et al., 2012) mice, indicating that cathepsin D can travel to lysosomes by Man-6-P-independent routes in this organ as well. The fact that mutations resulting in the inactivation or mislocalization of cathepsin D lead to neuronal ceroid lipofuscinosis, a neurodegenerative disease characterized by microcephaly, seizures, and cognitive and psychomotor defects (Tyynelä et al., 2000; Siintola et al., 2006; Steinfeld et al., 2006), suggests that these alternative pathways help support important cathepsin-D-dependent brain functions.

Our search for a putative cathepsin D transport receptor in mouse brain disclosed its binding to SEZ6L2, a type 1 transmembrane protein predominantly expressed in the brain (also known as BSRP-A, for brain-specific receptor A). Genetic variations in *SEZ6*, *SEZ6L* and *SEZ6L2* (the seizure-related gene 6 family) have been associated with febrile seizures, bipolar disorder I and autism (albeit the latter has not been confirmed in a subsequent study), respectively (Yu et al., 2007; Kumar et al., 2009; Mulley et al., 2011; Konyukh et al., 2011; Xu et al., 2013). Anti-SEZ6L2 antibodies have also been detected in a patient suffering from cerebellar ataxia and retinopathy (Yaguchi et al., 2014). Finally, it has been reported that mice deficient for all three SEZ6 members (Miyazaki et al., 2006) or for SEZ6 alone (Gunnersen et al., 2007) suffer from motor discoordination, cognitive defects and abnormal neuronal innervation, and that SEZ6 controls neuronal branching (Gunnersen et al., 2007). However, the roles of SEZ6L and SEZ6L2 are less well known, and the molecular mechanisms that mediate the action(s) of SEZ6 proteins in the brain are unclear.

We studied the intracellular trafficking and involvement of SEZ6L2 in cathepsin D sorting in HeLa cells and a neuroblastoma cell line (N1E-115), which revealed that SEZ6L2 travels to endosomes from the TGN and plasma membrane and is involved in the Man-6-P-independent transport of cathepsin D. Interestingly, we also found that the cleavage of SEZ6L2 by cathepsin D produces a soluble fragment that stimulates neurite outgrowth. These findings suggest that the SEZ6L2-mediated sorting of cathepsin D contributes to neural development, thereby shedding some long sought-after light on the importance of alternative pathways to Man-6-P-dependent trafficking in the brain.

RESULTS

Identification of SEZ6L2 as a new cathepsin-D-binding partner

To search for candidate Man-6-P-independent transport receptor(s) for cathepsin D in the brain, a detergent extract of a mouse brain membrane fraction (adjusted to pH 6.5) was first loaded onto a pepsinogen–Sepharose-4B affinity column. Pepsinogen shares 45% identity in amino acid composition with cathepsin D but is secreted rather than transported to lysosomes, suggesting that the alternative cathepsin D transport receptor(s) are unable to bind to

[1]URPhyM-Laboratoire de Chimie Physiologique, University of Namur, 61 rue de Bruxelles, Namur 5000, Belgium. [2]Department of Cell Biology, University Medical Center Utrecht, Heidelberglaan 100, Utrecht 3584 CX, The Netherlands.

*Author for correspondence (michel.jadot@unamur.be)

Received 19 August 2015; Accepted 17 December 2015

Journal of Cell Science (2016) 129, 557-568 doi:10.1242/jcs.179374

this protein (Baranski et al., 1990; Glickman and Kornfeld, 1993). The flow-through was then loaded on a cathepsin-D–Sepharose column (predominantly intermediate and two-chain forms of cathepsin D, with a lower amount of proforms). Proteins that bound to cathepsin D were eluted at acidic pH (4.5), as dissociation of receptor–ligand complexes trafficking to lysosomes generally takes place in acidified endosomes. These putative cathepsin-D-binding partners were then identified by mass spectrometry (see Materials and Methods and Fig. S1A–C for details), which revealed the single type 1 transmembrane protein named SEZ6L2. To validate this finding, we analyzed the elution profile of SEZ6L2 by western blotting after loading of the brain membrane extract directly on the cathepsin D column. SEZ6L2 (detected at ∼155 kDa) eluted after application of acidic conditions (pH 4.5), and further washing with a 1 M NaCl-containing buffer and a pH 3.5 glycine solution did not release any more of the protein (Fig. 1A). This elution profile was not observed when the sample was loaded on columns made of BSA, pepsinogen or acid alpha-glucosidase, another lysosomal hydrolase (Fig. 1A). Of note, SEZ6L2 bound optimally to cathepsin D at pH 6.5 and less efficiently at pH 7.4, whereas poor binding was observed at pH 8.0 (Fig. S1D). Finally, in accordance with the published report of a predominant neuronal expression of SEZ6L2 (Miyazaki et al., 2006), we mainly detected SEZ6L2 in the mouse brain, and found that it was expressed endogenously in a mouse neuroblastoma cell line (N1E-115) (Fig. 1B). Using the latter, we validated that SEZ6L2 could be co-immunoprecipitated with cathepsin D (Fig. S1E). Taken together, these findings support a specific interaction of SEZ6L2 with cathepsin D in neuronal cells.

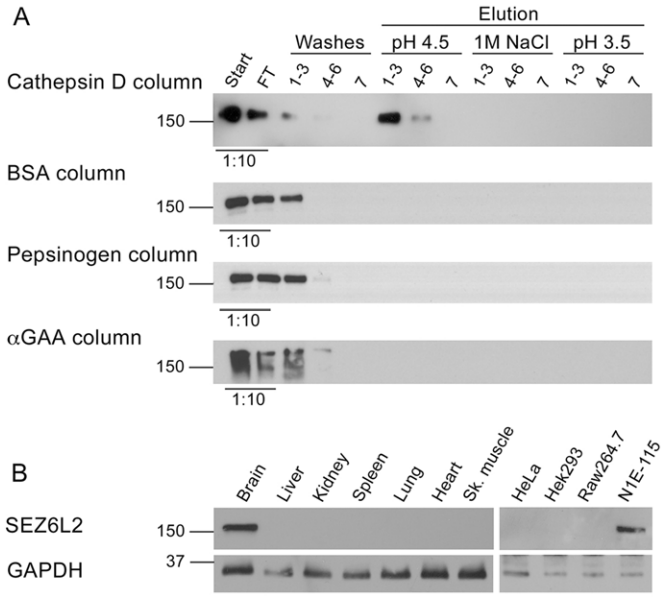

Fig. 1. Cathepsin D binds to the type 1 transmembrane protein SEZ6L2. (A) Loading of a brain membrane detergent extract on cathepsin D-, pepsinogen-, BSA-, or acid α-glucosidase (αGAA)-affinity columns at pH 6.5, followed by the detection of SEZ6L2 by western blotting in the flow-through (FT), the seven fractions collected during washing, and the fractions eluted after addition of buffer adjusted to pH 4.5, of buffer containing 1 M NaCl (pH 6.5) or of a glycine-NaCl solution at pH 3.5. The starting sample and flow-through are diluted 1:10 compared to the other fractions (which were precipitated with TCA). (B) Detection of SEZ6L2 by western blotting in mouse organs and in human (HeLa and Hek293) or mouse (Raw264.7 and N1E-115) cell lines. GAPDH was used as a loading control.

SEZ6L2 travels to endosomes but does not reach lysosomes

As a first step to investigate the putative role of SEZ6L2 in the endolysosomal transport of cathepsin D, we followed its subcellular trafficking. Transfection of HeLa cells with mouse *Sez6l2* fused to a MYC tag at its C-terminal end and immunoblotting with an anti-SEZ6L2 antibody directed against the N-terminal portion or with an anti-MYC antibody (see schematic in Fig. S1C) revealed two SEZ6L2 forms, of ∼140 kDa and 155 kDa (Fig. 2A). Similar results were obtained in transfected N1E-115 neuroblastoma cells, in which SEZ6L2 is expressed endogenously (Fig. 2B). Metabolic labeling with [^{35}S]Met/Cys and endoglycosidase treatments to follow the processing of SEZ6L2 over time revealed that the 140-kDa form is synthesized first and that it bears high-mannose oligosaccharidic chains which, over time, are progressively converted into larger complex-type structures (Fig. S1F). This indicates that SEZ6L2 travels through the Golgi, where conversion of glycans into complex structures takes place. Our results also suggest that some O-glycosylation can occur on the protein. These modifications raise the relative migration of SEZ6L2 to ∼155 kDa.

Next, we analyzed the subcellular localization of SEZ6L2 in transfected HeLa cells by immunofluorescence. Permeabilized conditions highlighted a cytosolic and perinuclear punctate staining (Fig. 2C). Without permeabilization, a cell surface staining was detected with the anti-SEZ6L2 antibody, but not with the anti-MYC antibody, indicating that the N-terminal moiety of SEZ6L2 is extracellular, whereas its C-terminal tail faces the cytosol. Colocalization studies with different markers were then conducted in permeabilized cells. The endolysosomal membrane protein LAMP-2 was partially colocalized with SEZ6L2, as reflected by a Pearson's correlation coefficient (PCC) of 0.47±0.02 (mean± s.e.m., n=85). Lower colocalization was seen between cathepsin D and SEZ6L2 (detected with anti-MYC antibody) (PCC=0.22±0.02, n=41). However, it should be noted that the colocalization of cathepsin D and LAMP-2 in HeLa cells is not complete (Fig. S2, PCC=0.73±0.01, n=36), in accordance with the fact that LAMP-2 labels endosomes and lysosomes whereas cathepsin D, although being present in endosomes, mainly resides in lysosomes (Rijnboutt et al., 1992). In addition, SEZ6L2 colocalized with Vps26, a subunit of the retromer complex that recycles cargo from endosomes to the TGN (PCC=0.61±0.02, n=32), and with CI-MPR (also known as IGF2R), which mainly localizes to the TGN, early and late endosomes (PCC=0.63±0.01, n=67) (Fig. 2C). Similarly, we observed that endogenous SEZ6L2 in N1E-115 cells partly localizes to the plasma membrane and colocalizes with LAMP-2 (PCC=0.63±0.02, n=57), Vps26 (0.68±0.02, n=32) and CI-MPR (0.60±0.03, n=29) [Fig. 2D and Fig. S2 show the loss of SEZ6L2 signal in N1E-115 cells treated with small interfering RNAs (siRNAs) targeting *Sez6l2*]. Owing to cross-reactivity, the colocalization of endogenous SEZ6L2 with cathepsin D could not be tested in these cells.

Taken together, these results indicate that SEZ6L2 traffics to endosomes but that very little of the protein reaches lysosomes, most likely due to rapid recycling of the protein to the TGN and/or plasma membrane.

Tyrosine-based signals mediate the transport of SEZ6L2 to endosomes via clathrin-coated vesicles

Clathrin-coated vesicles (CCVs) are known to transport their cargos, including complexes between lysosomal hydrolases and MPRs, from the TGN or plasma membrane to endosomes. We found a 4.9±1.3-fold (mean±s.d., n=3) enrichment of SEZ6L2 in a CCV fraction prepared from mouse brain (i.e. enriched in CCV coat

Journal of Cell Science (2016) 129, 557-568 doi:10.1242/jcs.179374

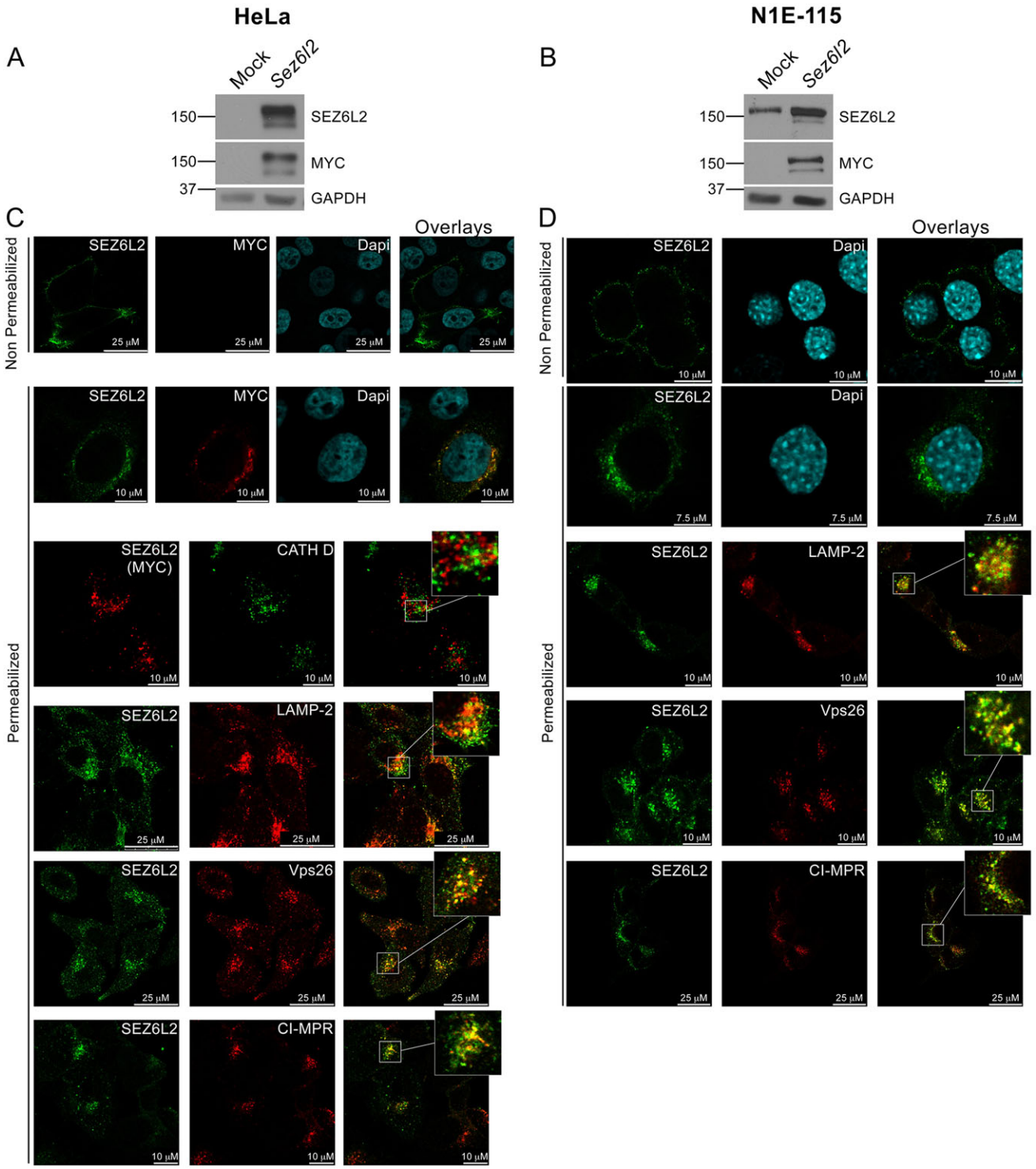

Fig. 2. SEZ6L2 localizes to endosomes and plasma membrane and colocalizes with proteins that cycle between endosomes and TGN. HeLa (A) and N1E-115 (B) cells were transiently transfected with *Sez6l2*–MYC for 48 h prior to detection of SEZ6L2 by western blotting using anti-SEZ6L2 (against the N-terminal region) or anti-MYC (against the C-terminal region) antibodies. GAPDH was used as a loading control. The subcellular localization of SEZ6L2–MYC overexpressed in HeLa cells (C) or of SEZ6L2 endogenously expressed in N1E-115 cells (D), was then analyzed by immunofluorescence. The presence of SEZ6L2 at the plasma membrane was assessed in the absence of permeabilization, whereas colocalization studies with markers of late endosomes and lysosomes (LAMP-2), of lysosomes (cathepsin D) and with two proteins that cycle between endosomes and TGN (CI-MPR and the retromer component Vps26), were conducted under permeabilized conditions. In the upper panels, DAPI was used to highlight nuclei.

components, including the plasma membrane clathrin adaptor AP-2, and in CI-MPR, but not in proteins that do not traffic through CCVs, such as cytochrome *c*, GAPDH and Sec61) (Fig. 3A; CCV fraction diluted 8× compared to the starting homogenate). Moreover, the transfection of HeLa cells with SEZ6L2–MYC–FLAG followed by the detection of SEZ6L2 by immunoelectron

Journal of Cell Science (2016) 129, 557-568 doi:10.1242/jcs.179374

microscopy with an anti-FLAG antibody validated the presence of SEZ6L2 in CCVs, in addition to its localization at the plasma membrane and in endosomes (Fig. 3B).

The short cytosolic tail of SEZ6L2 (see schematic in Fig. S1C) contains a putative CCV-packaging motif of the Yxxϕ-type (Y^{897}SPI), a consensus sequence notably recognized at the TGN and plasma membrane by the CCV adaptor proteins, AP-1 and AP-2, respectively. SEZ6L2 also contains a putative endocytosis motif of the NPxY-type ($NPLY^{911}$), a sequence recognized by several plasma membrane clathrin adaptors including AP-2 and Dab2. To test the putative role of these motifs in the transport of SEZ6L2, we mutated their crucial tyrosine residues to alanine. First, we measured the cell surface level of the Yxxϕ (Y897A), NPLY (Y911A) or double (Y897A+Y911A) mutants expressed in HeLa cells using cell surface biotinylation. This experiment revealed that, at steady state, 11±3% of wild-type SEZ6L2 resided at the plasma membrane (Fig. 3C). This level increased significantly to 16±4%, and to 16±6% when the Yxxϕ or NPxY motifs were mutated, respectively ($n \geq 5$, $P<0.05$). The cell surface level reached 32±10% when both motifs were mutated simultaneously ($P<0.01$). These results demonstrate that both motifs are required for efficient trafficking of SEZ6L2 in transfected HeLa cells. Similarly, we found that both motifs mediate the transport of SEZ6L2 in N1E-115 cells (Fig. S2C). Of note, in those cells, the Y897A mutation induced a higher increase of cell surface level than the Y911A mutation, suggesting that the Yxxϕ motif plays a more predominant role in the sorting of SEZ6L2 than the NPxY motif in neuronal cells.

Next, we used ^{125}I-labeled anti-SEZ6L2 antibodies to mark the plasma membrane pool of the different mutants and monitor their internalization. We found that mutation of the NPxY motif, but not of the Yxxϕ motif, severely reduced the uptake of SEZ6L2 by HeLa cells; that is, the intracellular levels of the Y911A and Y897A+Y911A mutants were fourfold lower (after 90 min internalization at 16°C) than those of wild-type and the Y897A mutant (Fig. 3D). In addition, pulldown assays performed using the C-terminal tail of SEZ6L2 fused to GST showed that the NPxY, but not the Yxxϕ signal, mediated interaction of SEZ6L2 with Dab2-containing endocytic complexes (Fig. 3E).

Finally, although no interaction could be detected between SEZ6L2 and the TGN or endosomal clathrin adaptor AP-1 by GST pulldown (data not shown), immunofluorescence analyses revealed a partial colocalization between this adaptor and wild-type SEZ6L2 (Fig. 3F, PCC=0.54±0.02, mean±s.e.m., n=28). Moreover, whereas a similar colocalization level was detected between the Y911A mutant and AP-1 (PCC=0.49±0.03, n=28), the overlap with this adaptor significantly decreased for SEZ6L2 proteins bearing the Y897A mutation (PCCs=0.37±0.03 and 0.34±0.03 for the Y897A and Y897A+ Y911A mutants, respectively, n=28, $P<0.001$). The double mutant Y897A+Y911A exhibited the most striking elevation of plasma membrane residency, in accordance with the biotinylation analysis, and we observed that only a very small amount of this mutant reached LAMP-2-positive compartments (Fig. S2D). Combined with the results of biotinylation, internalization and pulldown experiments, these findings indicate that the NPxY motif serves as an endocytosis signal, and that the Yxxϕ motif works at an intracellular site, possibly as a TGN and/or endosomal exit signal. In contrast to the NPxY mutant, which accumulates at the plasma membrane due to a decreased internalization from this site, the increase of cell surface level of the Y897A mutant is likely the result of its escape from packaging at the TGN into CCVs bound to endosomes and/or the consequence of an increase of its recycling from endosomes to the plasma membrane. The lack of interaction between the Yxxϕ motif and AP-1 in our pulldown assay might result from technical limitations, or point to the involvement of a different adaptor in the recognition of this signal for packaging in CCVs.

Knockdown of *Sez6l2* in N1E-115 cells impacts on the trafficking of cathepsin D

To test whether SEZ6L2 is involved in the transport of cathepsin D, we knocked down its expression using a pool of four siRNAs in mouse N1E-115 cells (Fig. 4A–C). As the processing of cathepsin D from proform to intermediate and two-chain forms is indicative of arrival in endosomes and lysosomes, we measured, by western blotting, the intracellular levels of the different forms of cathepsin D at 48 h post-transfection with control and *Sez6l2* siRNAs. At steady state, no significant differences of processing were observed in SEZ6L2-deficient cells versus control cells (Fig. 4A; Table S1A). However, the amount of ^{125}I-labeled recombinant mouse procathepsin D captured by SEZ6L2-deficient cells after a 30-min incubation period at 37°C (in the presence of Man-6-P to block MPR-mediated capture) decreased by almost 20% compared to control cells (Fig. 4B, $P<0.05$), suggesting that SEZ6L2 is involved in the endocytosis of this protease. In addition, a 30-min pulse labeling with [^{35}S]Met/Cys, followed by a 4 h chase in unlabeled medium supplemented with Man-6-P to saturate cell surface MPRs, highlighted a significant increase of cathepsin D in the medium of SEZ6L2-deficient cells (26±16% of the total labeled cathepsin D forms) compared to control cells (13±8%) (mean±s.d., n=4, ~twofold increase, $P<0.05$, Fig. 4C). This increase was also observed with two individual siRNAs selected from the pool (resulting in a >90% reduction of SEZ6L2 expression), which reduces the likelihood of an off-target effect on cathepsin D sorting (Fig. S3A,B). In these pulse–chase experiments, the decreased endocytosis of procathepsin D by SEZ6L2-deficient cells might slightly increase its presence in the extracellular medium. However, under cell culture conditions, it should be noted that only low amounts of procathepsin D (diluted in extracellular medium) are captured by SEZ6L2-mediated endocytosis. It seems unlikely, therefore, that the loss of this process could, by itself, account for the increased extracellular procathepsin D level observed upon silencing of *Sez6l2*. As the cathepsin D mRNA levels (measured by qRT-PCR) were not affected by the loss of SEZ6L2 (data not shown), this increase likely reflects the secretion of cathepsin D proforms that escaped the cells through the constitutive secretory pathway due to the absence of SEZ6L2 at the TGN to transport them to endolysosomes. The finding that SEZ6L2 Yxxϕ motif is recognized at an intracellular site (not at the plasma membrane) and the observation that the optimum pH for binding of cathepsin D to SEZ6L2 is 6.5 are consistent with this view.

Transient expression of SEZ6L2 in HeLa cells with a deficient Man-6-P pathway partially corrects cathepsin D missorting

The limited impact of *Sez6l2* silencing on cathepsin D sorting in N1E-115 cells suggests that other transport receptors (including Man-6-P receptors) might compensate for the loss of SEZ6L2 in those cells. Here, we used a cell type unable to retain cathepsin D in the absence of a functional Man-6-P pathway to further investigate the putative role of SEZ6L2 in the subcellular trafficking of this hydrolase. Although very low levels of cathepsin D could be detected in the culture medium of control HeLa cells, the CRISPR–Cas9-mediated inactivation of the first enzyme involved in Man-6-P synthesis (Ptase) induced procathepsin D hypersecretion by those

Journal of Cell Science (2016) 129, 557-568 doi:10.1242/jcs.179374

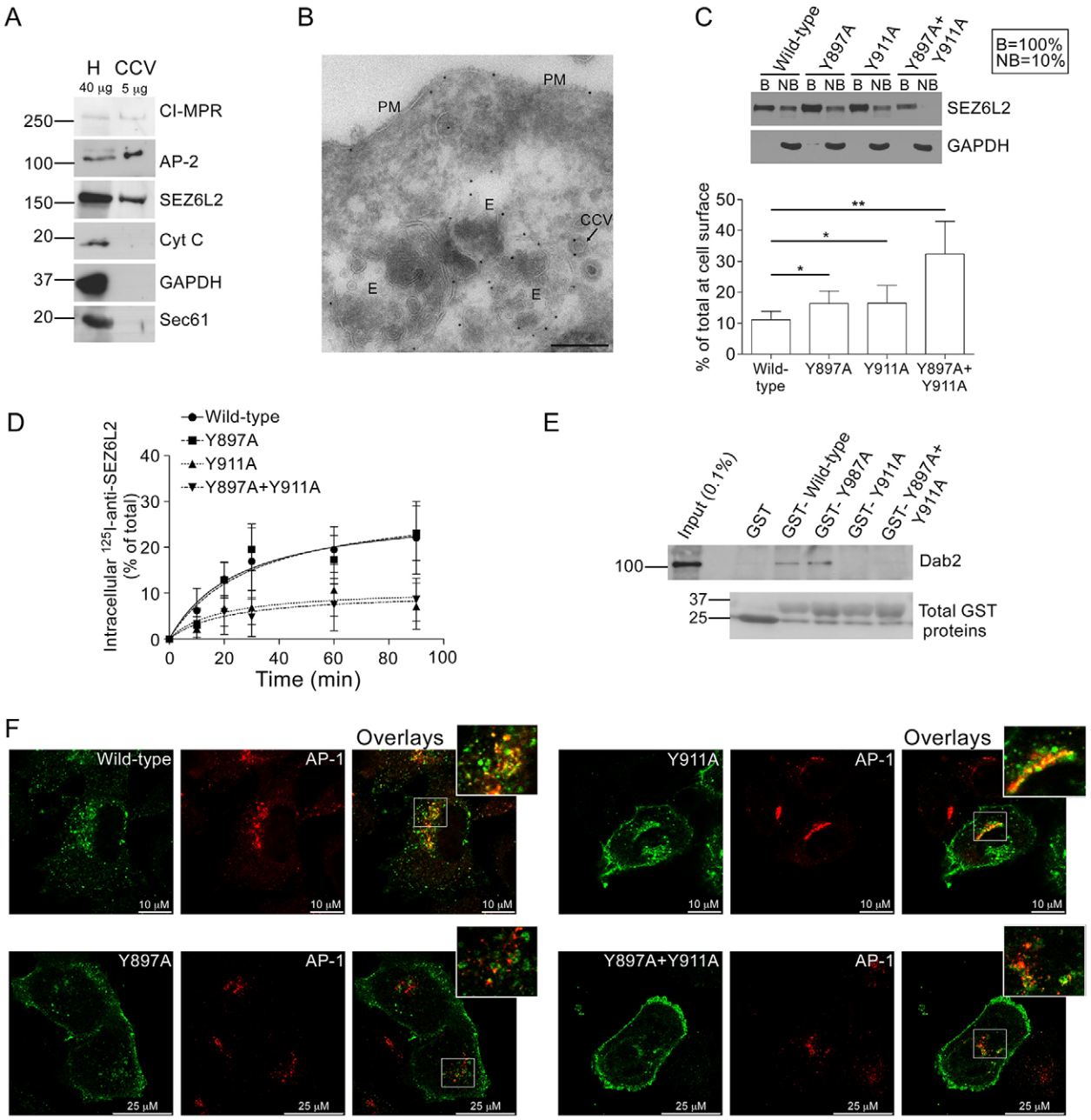

Fig. 3. Two sorting signals mediate the transport of SEZ6L2 to endosomes via CCVs. (A) Western blotting detection of SEZ6L2, clathrin adaptor protein AP-2 and CI-MPR in a mouse brain fraction enriched in CCVs (5 µg of proteins loaded) compared to the starting brain homogenate (H, 40 µg of proteins). One representative experiment is shown (total n=3 independent experiments). Several proteins that do not travel through CCVs were used as negative controls (mitochondrial cytochrome c, cytosolic GAPDH and endoplasmic reticulum Sec61β). (B) Detection of SEZ6L2–MYC–FLAG 48 h post-transfection in HeLa cells by immunoelectron microscopy, using an anti-FLAG antibody. E, endosome; PM, plasma membrane. The arrow points to a CCV. Scale bar: 200 nm. (C) Measurement of the plasma membrane level of SEZ6L2 mutants in transfected HeLa by a cell surface biotinylation method, after mutation of its C-terminal Y^{897}SPI and NPLY^{911} motifs. Tyrosine residues were replaced by alanine (Y897A and Y911A, respectively). GAPDH was used as a control of cell impermeability to the biotinylation reagent. Note that only 10% of the non biotinylated fraction (NB) was loaded on gel compared to the biotinylated (B) fraction. The SEZ6L2 signals detected in each fraction were quantified and are shown on the graphs (mean±s.d., $n\geq5$ independent experiments per construct). *P<0.05, **P<0.01 (non-paired, two-tailed Student's t-test). (D) Internalization assay. ^{125}I-labeled anti-SEZ6L2 antibodies were bound to cell surface SEZ6L2 for 30 min at 4°C, followed by incubation at 16°C for 10, 20, 30, 60 and 90 min. The radioactivity counted in cell lysates collected at each time points, after removal of the remaining cell surface-bound antibodies, is expressed as a percentage of the total bound radioactivity after the 30 min binding period at 4°C (mean±s.d., n=6). (E) Test of the interaction of the C-terminal tail of SEZ6L2 (wild-type or with Y897A and/or Y911A mutations) fused to GST with the endocytic adaptor Dab2 in a HeLa cell lysate. Loading controls for GST-tagged proteins are also shown. (F) Detection by immunofluorescence of the TGN and endosomal clathrin adaptor AP-1 and of SEZ6L2 (wild-type or mutated) 48 h post-transfection in HeLa cells.

cells (Fig. 4D). An increase of the total level of cathepsin D was also detected in the knockout cells, likely reflecting upregulation of lysosomal genes in answer to lysosomal dysfunction (Sardiello et al., 2009). Transfection of wild-type *Sez6l2* in control cells did not alter cathepsin D sorting (as indicated by a similar processing of the enzyme in transfected and control cells), likely due to the

Journal of Cell Science (2016) 129, 557-568 doi:10.1242/jcs.179374

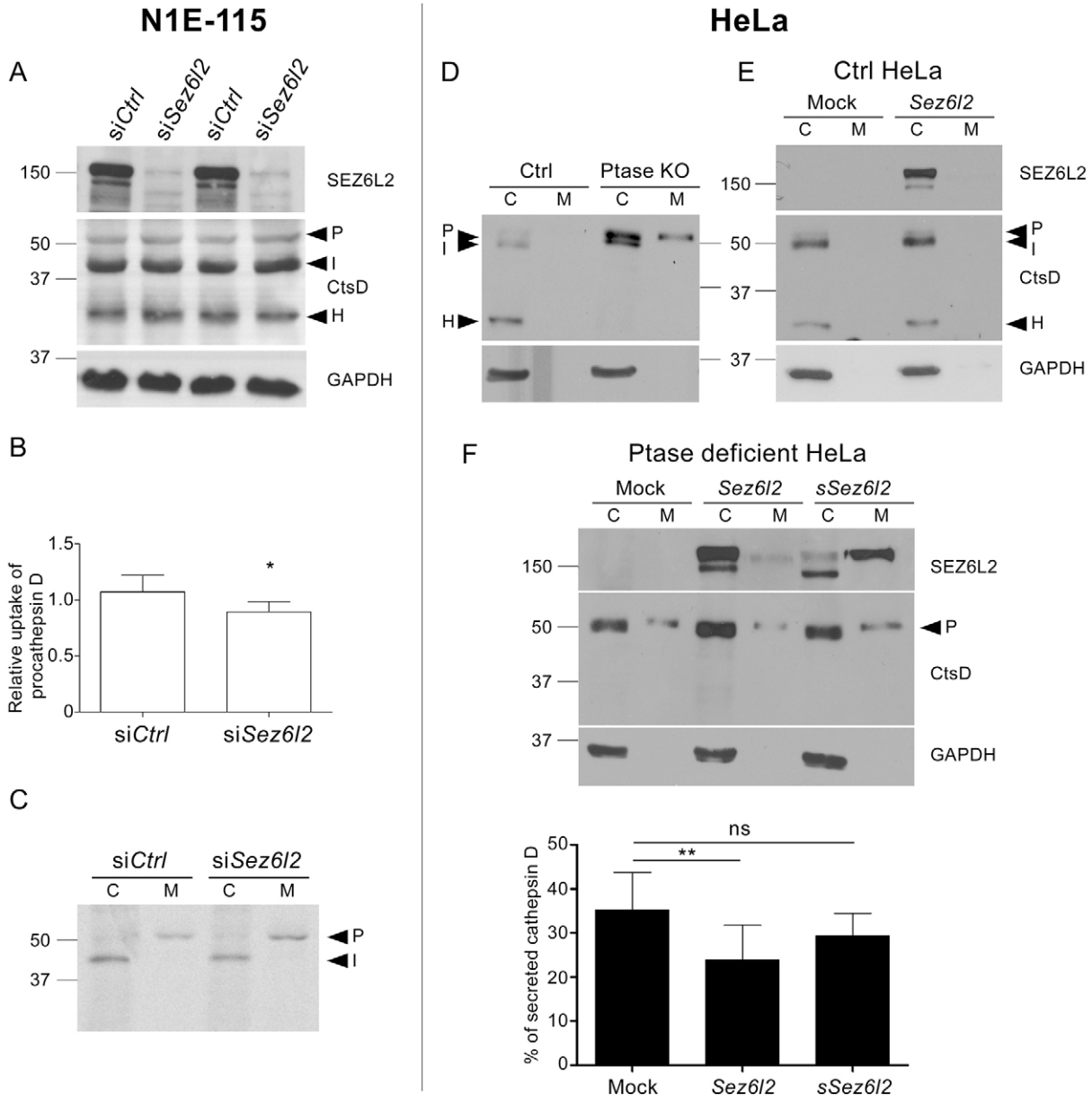

Fig. 4. SEZ6L2 can modulate the intracellular sorting of cathepsin D. (A) Steady state levels of SEZ6L2 and of the different forms of cathepsin D (P, precursor; I, intermediate; H, heavy chain) after treatment with control siRNAs (si*Ctrl*) or siRNAs against *Sez6l2* (si*Sez6l2*; pool of four siRNAs) in N1E-115 cells. GAPDH was used as a loading control. Two individual sets are shown. Quantifications of the ratios of cathepsin D forms in n=9 independent experiments are provided in Table S1. (B) Comparison of the relative amount of radioactivity captured by si*Ctrl*- and si*Sez6l2*-treated N1E-115 cells after 30 min at 37°C in the presence of ^{125}I-labeled procathepsin D and 5 mM Man-6-P (mean±s.d., n=3 independent experiments). *P<0.05 (non-paired, two-tailed t-test). (C) Immunoprecipitation of cathepsin D from si*Ctrl*- and si*Sez6l2*-treated cell lysates (C) and media (M) collected after a 30-min pulse labeling with [^{35}S]Met/Cys and a 4-h chase in unlabeled medium containing 5 mM Man-6-P. One representative experiment is shown. The level of procathepsin D in the culture medium was estimated from n=4 independent experiments [13±8% and 26±16% (mean±s.d.) in si*Ctrl*- and si*Sez6l2*-treated cells, respectively (P<0.05, two-tailed t-test)]. (D) Detection of cathepsin D in control and Ptase-knockout (KO) HeLa cell lysates and culture media (collected after 5 h in serum-free medium). GAPDH is used as loading control. Note that after PNGase F treatment of a Ptase-KO cell lysate, a single form of 48 kDa is detected, suggesting that the intracellular doublet mainly contains cathepsin D proforms (data not shown). (E,F) Detection of SEZ6L2, cathepsin D and GAPDH by western blotting in mock- or *Sez6l2*-transfected control (E) or Ptase-deficient (F) HeLa cell lysates and culture media collected after a 5 h culture in serum-free conditions (48 h post-transfection). *sSez6l2* in F indicates expression of the N-terminal portion of SEZ6L2 (highly secreted or soluble SEZ6L2). The graph in F shows the proportion of cathepsin D secreted by Ptase-deficient cells (mean±s.d., n≥5 independent experiments). **P<0.01, non-paired, two-tailed t-test; ns, not significant.

presence of an efficient Man-6-P sorting pathway (Fig. 4E; see Table S1B for detailed quantifications). However, the level of procathepsin D secreted by Ptase deficient cells significantly decreased from 35±8% to 24±8% when wild-type SEZ6L2 was overexpressed (Fig. 4F, P<0.01). Taking into account a transfection efficiency of 36±14% in the Ptase-deficient cells, this 32% decrease suggests that overexpression of SEZ6L2 markedly affects the secretion of cathepsin D by those cells. By contrast, expression of the soluble N-terminal domain of SEZ6L2 (sSEZ6L2), which lacks the transmembrane domain and C-terminal tail containing the endosomal sorting signals, and is secreted as a result, only induced a slight, and non-significant decrease, of cathepsin D secretion. It is

Journal of Cell Science (2016) 129, 557-568 doi:10.1242/jcs.179374

also worth noting that the intracellular retention of cathepsin D induced by wild-type SEZ6L2 was not accompanied by the appearance of cathepsin D heavy chain inside the Ptase-deficient cells. This might be due to the missorting of some other proteases required for cathepsin D processing (Laurent-Matha et al., 2006) and/or be a consequence of the abnormal storage of undegraded material in lysosomes, which might impair enzyme maturation (Hamer and Jadot, 2005). Nevertheless, given that this retention is more pronounced after expression of the SEZ6L2 protein that traffics to endosomes, as opposed to the soluble form that only transits through biosynthetic compartments before being secreted, our findings indicate that membrane-bound SEZ6L2 can act as an alternative to the Man-6-P receptor for procathepsin D sorting to endosomes or lysosomes.

The morphology of N1E-115 cells is modulated by SEZ6L2 and cathepsin D

An increase of dendritic arborisation of mouse cortical neurons has been reported upon knockout of *Sez6*, the first identified member of the gene family to which *Sez6l2* belongs to (Gunnersen et al., 2007). That study also showed that the membrane-bound and a secreted isoform of SEZ6 had opposite anti- and pro-branching activity, respectively. Interestingly, when we investigated the presence of SEZ6L2 in the culture medium of HeLa cells transfected with wild-type SEZ6L2–MYC, we detected low amounts of a secreted form of the protein, with a slightly lower molecular mass compared to the 155-kDa intracellular from (Fig. 5A). A 30-min pulse (with [^{35}S]Met/Cys) and 4 h chase followed by immunoprecipitation using the anti-SEZ6L2 antibody (against the N-terminal part) or anti-MYC antibody (against the C-terminal part), revealed that the secreted form (sSEZ6L2) had lost its MYC tag (Fig. 5B). This strongly suggests that cells can produce sSEZ6L2 by proteolytic cleavage of the transmembrane-domain-containing C-terminal portion of SEZ6L2. We wondered whether this cleavage also took place endogenously in neuroblastoma cells, and whether cathepsin D could be involved. To test this, we measured the amount of endogenous sSEZ6L2 produced (after a 30-min pulse and 4-h chase) by mock-transfected N1E-115 cells, and cells transfected with wild-type procathepsin D or its inactive mutant D295N (Fig. 5C). We found that N1E-115 cells secreted sSEZ6L2 and that overexpression of wild-type procathepsin D, but not D295N procathepsin D, significantly raised sSEZ6L2 secretion to 17±3% (of total SEZ6L2), compared to 11±1% in mock-transfected cells (P<0.001). Moreover, the addition of the aspartic protease inhibitor pepstatin A significantly decreased the level of sSEZ6L2 produced by the mock-transfected cells, and prevented the increase of secretion induced by the overexpression of cathepsin D (P<0.01). These results strongly support that cathepsin D is involved in the proteolytic cleavage of membrane SEZ6L2, which results in the release of a large N-terminal fragment (sSEZ6L2). As membrane-bound SEZ6L2 does not travel to lysosomes, cleavage likely occurs in endosomes, in which cathepsin D-mediated degradation has been reported (Diment and Stahl, 1985; Authier et al., 1995). Of note, some sSEZ6L2 might also be produced by other proteases. It has been found that SEZ6L2 is a substrate of the aspartic proteases BACE1 and BACE2 (β-secretases) in neurons and pancreatic β-cells, respectively (Stützer et al., 2013, Kuhn et al., 2012).

Next, we investigated whether membrane-bound SEZ6L2 and its soluble fragment could, similarly to the membrane and soluble SEZ6 forms, exhibit anti-and pro-neuronal differentiation properties, respectively. Interestingly, after knockdown of *Sez6l2* using a pool of four siRNAs, N1E-115 cells underwent drastic

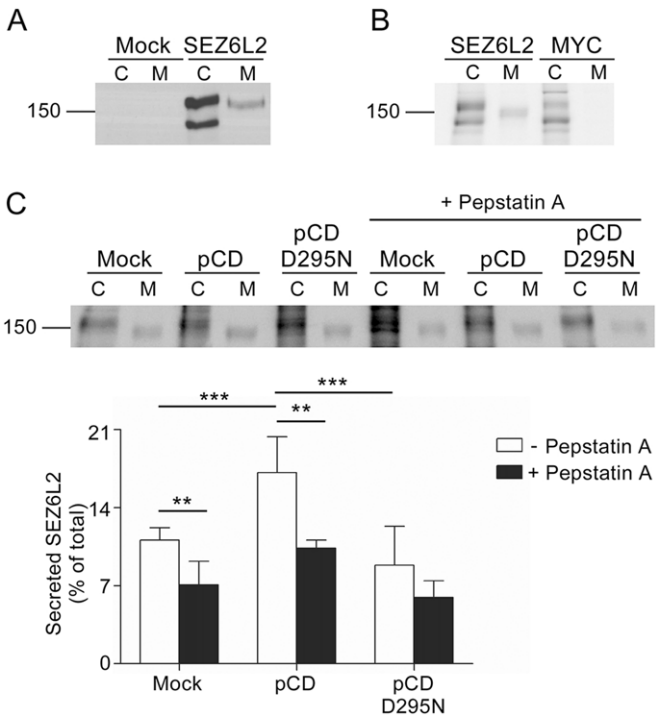

Fig. 5. Cathepsin D is able to generate a soluble fragment of SEZ6L2. (A) Detection of SEZ6L2 by western blotting in HeLa cell lysates (C) and media (M) collected 48 h after transfection with pcDNA3.1 (Mock) or pcDNA3.1-*Sez6l2*-MYC (SEZ6L2). The medium samples were collected after 5 h culture in serum-free conditions. Note that medium samples are concentrated 2× compared to cell lysates. (B) Immunoprecipitation of SEZ6L2 from HeLa cell lysates and medium collected after a 30-min pulse with [^{35}S]Met/Cys and a 4-h chase, using anti-SEZ6L2 and -MYC antibodies. (C) Measurement of the amount of sSEZ6L2 secreted by N1E-115 cells transfected with procathepsin D (pCD) or procathepsin D D295N (inactive). Soluble and membrane SEZ6L2 were immunoprecipitated from the cells (C) and their culture medium (M) was collected after a 30-min pulse with [^{35}S]Met/Cys and a 4-h chase. When indicated, the inhibitor pepstatin A was added during the 4-h chase period. After SDS-PAGE, the radioactive signals were detected with a Cyclone™ Phosphor Imager and quantified (taking into account background noise) with OptiQuant™. Results are mean±s.d. (n≥3 independent experiments). **P<0.01, ***P<0.001 (non-paired, two-tailed t-test).

morphological changes, with loss of their regular round shape, enlargement of cell bodies and appearance of neurites that were reminiscent of an enhanced neuronal differentiation (Fig. 6A). The proportion of cells exhibiting these changes increased from 3.1±0.4% in control cells to 11.6±1.6% in SEZ6L2-deficient cells (P<0.001) (Fig. 6A,B). A significant increase, ranging from 7.3±1.4 to 11.9±2.8, was also observed with individual siRNAs of the pool (Fig. S3C,D). Of note, re-expression of membrane SEZ6L2 (24 h after treatment with the pool of siRNAs), resulted in a significant reduction of the percentage of neurite-bearing cells (Fig. 6C, P<0.05), whereas expression of the soluble form of SEZ6L2 lacking its transmembrane domain and C-terminal tail (sSEZ6L2) had no significant inhibitory impact (Fig. 6C).

The overexpression of sSEZ6L2, but not SEZ6L2, in non-differentiated N1E-115 cells induced a significant increase (of 43±25%) in the number of enlarged cells that had lost their round shape and had short neurites (P<0.05) (Fig. 7A,B; see Fig. S4 for transfection controls). Similarly, the addition of conditioned medium from HeLa cells transfected with sSEZ6L2 (collected 48 h after removal of the transfection medium) resulted in a 40±12% increase of short-neurite-bearing N1E-115 cells, compared to cells incubated

Journal of Cell Science (2016) 129, 557-568 doi:10.1242/jcs.179374

with medium collected from mock-transfected HeLa cells ($P<0.05$) (Fig. 7C). Taken together, these findings suggest that there is a pro-differentiation effect of the secreted form of SEZ6L2, and support that siRNA knockdown of all forms of SEZ6L2 (Fig. 6) induces neurite outgrowth by preventing inhibition by the predominant membrane form, taking precedence over the loss of sSEZ6L2.

Finally, knowing that cathepsin D can regulate the production of sSEZ6L2, we investigated the impact of this protease on the morphology of N1E-115. Transient expression of wild-type cathepsin D induced a twofold increase of the number of cells bearing short neurites (Fig. 7D, $P<0.001$), whereas transfection with the D295N mutant (correctly targeted but inactive), glycopepsinogen (which is not sorted to lysosomes), or with a procathepsin D form fused to an endoplasmic reticulum retention signal (KDEL) to prevent its transport and processing into endolysosomes, had no impact. Controls of the expression and processing of the different constructs are provided in Fig. S4. An increase was also observed when the cells were incubated with conditioned medium collected from HeLa cells transfected with procathepsin D, but not when incubated with D295N- or glycopepsinogen-enriched medium (Fig. 7E). These results indicate that cathepsin D can influence neuronal morphology and that this action is dependent upon its correct intracellular trafficking and activation. Combined with the observation that overexpression of cathepsin D increases the level of sSEZ6L2, which is a promoter of neurite growth, these findings suggest that cathepsin D can promote neuronal differentiation through shedding of sSEZ6L2 molecules.

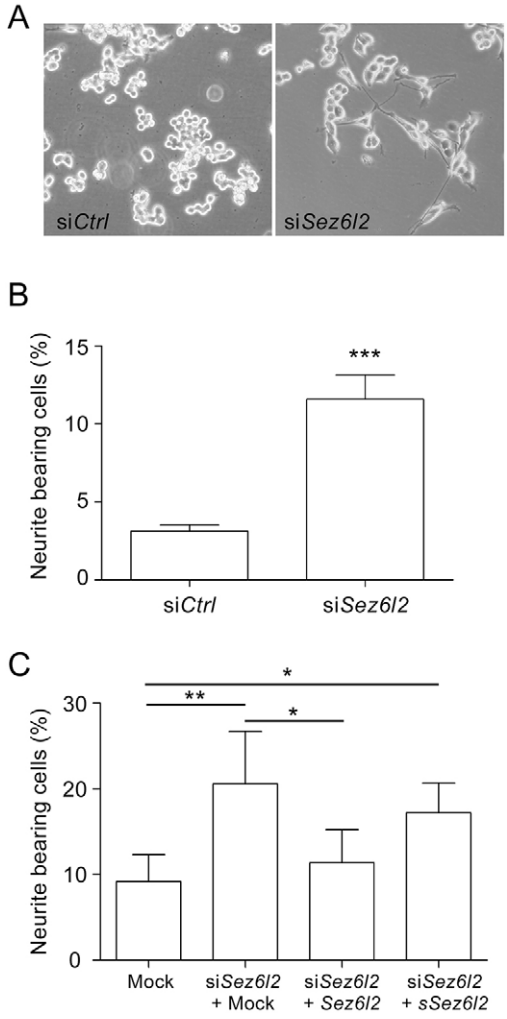

Fig. 6. Silencing of *Sez6l2* induces neurite outgrowth. (A) Effect of *Sez6l2* knockdown with a pool of siRNAs (si*Sez6l2*) on the morphology of N1E-115 cells (i.e. loss of round shape, appearance of neurites) observed by phase-contrast microscopy. (B) Counting of cells exhibiting an altered morphology (see Materials and Methods for details), expressed as percentage of total cells (mean±s.d., five independent experiments). ***$P<0.001$ (non-paired *t*-test, two-tailed). (C) The cells were transfected with *Sez6l2* siRNAs for 24 h, then for 24 h with mock (empty plasmid), *Sez6l2*-or *sSez6l2*-coding plasmids, prior to counting of cells exhibiting morphological changes (mean±s.d., $n=5$) *$P<0.05$, **$P<0.01$ (one-way ANOVA followed by Bonferroni's multiple comparison tests). Only significant differences are shown on the graph.

DISCUSSION

Several lysosomal soluble proteins, including cathepsin D, can use alternatives to the Man-6-P-dependent routes to reach endolysosomes, but very few of these alternative pathways have been identified so far. β-glucocerebrosidase, a non-phosphorylated enzyme, uses the lysosomal membrane protein LIMPII as a transport receptor (Reczek et al., 2007). Sortilin is involved in the sorting of prosaposin, GM2AP, acid sphingomyelinase, cathepsin H and cathepsin D in selected cell types (Lefrancois et al., 2003; Canuel et al., 2008; Wähe et al., 2010) and, in fibroblasts, cathepsin B and D can be captured by the membrane proteins LRP1 and LDLR (Derocq et al., 2012; Markmann et al., 2015). We now report a role of the type 1 transmembrane protein SEZ6L2 in the Man-6-P-independent transport of cathepsin D in neurons. This alternative receptor, which was the more abundant cathepsin D-binding partner found in the mouse brain membrane fraction used in our affinity purification experiment, might explain, at least partly, the normal levels and processing of cathepsin D observed in the brain of Ptase-deficient mice (unpublished data from Boonen et al., 2011; Kollmann et al., 2012). Interestingly, our findings suggest that both SEZ6L2-mediated and Man-6-P-dependent sorting of cathepsin D are active in neurons. This might reflect the need for a tight regulation of cathepsin-D-mediated protein clearance and/or the involvement of this protease in a broader spectrum of neuronal processes. A relevant example of protein that accumulates as a consequence of cathepsin D deficiency is α-synuclein, a protein involved in the formation of Lewy bodies in Parkinson and other neurodegenerative diseases, which demonstrates the importance of maintaining efficient cathepsin-D-mediated protein degradation in the brain (Sevlever et al., 2008; Cullen et al., 2009). In addition, we found that cathepsin D processes SEZ6L2 into a soluble fragment (sSEZ6L2), which is released in the extracellular medium, possibly after exocytosis of the endolysosomes. This fragment exhibits a neuronal pro-differentiation action, whereas the membrane form has the opposite effect, revealing that modulation of the ratio of sSEZ6L2 to SEZ6L2 forms mediated by cathepsin D provides a regulation mechanism of neuronal differentiation. Animal models and human patients bearing mutations in the cathepsin D gene that impair the activity, stability or trafficking of the enzyme (i.e. which cause neuronal ceroid lipofuscinosis), could exhibit alterations of the SEZ6L2 to sSEZ6L2 ratio, possibly leading to some of the pathological manifestations of the disease, which include seizures (Steinfeld et al., 2006; Siintola et al., 2006; Tyynelä et al., 2000; Koike et al., 2000; Koch et al., 2011, 2013). In this regard, it is interesting to note that mice with knocked out *Sez6* (the first member of the seizure-related gene family) exhibit a higher resistance to induced seizures (Gunnersen et al., 2007).

The mechanisms by which sSEZ6 (Gunnersen et al., 2007) and sSEZ6L2 favor neurite outgrowth, whereas their membrane forms

Journal of Cell Science (2016) 129, 557-568 doi:10.1242/jcs.179374

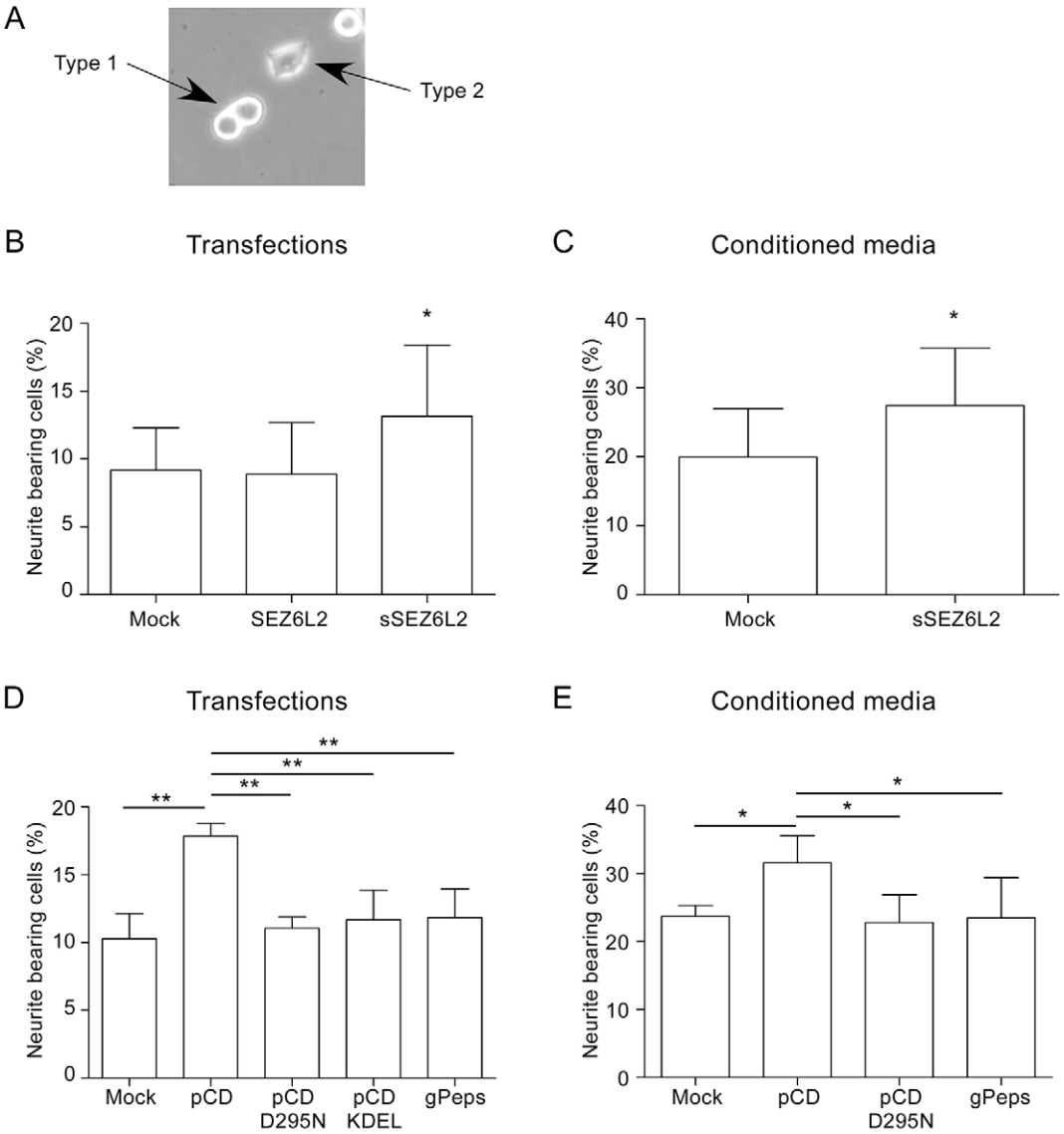

Fig. 7. sSEZ6L2 and procathepsin D modulate neuronal morphology. (A) Representative morphologies of N1E-115 cells in this experiment: round shaped with no neurite projections (morphology type 1) or exhibiting signs of neurite growth (morphology type 2, i.e. increase of cell body volume, loss of round shape, and presence of short neurites). (B) Effect of the overexpression of SEZ6L2 (membrane form) or sSEZ6L2 (soluble form) on N1E-115 cell morphology. (C) Incubation of N1E-115 cells for 24 h with conditioned medium enriched in sSEZ6L2 (collected from HeLa cells transfected with *sSez6l2*) and measurement of the percentage of cells exhibiting morphological changes, compared to cells incubated with medium collected from mock-transfected cells. (D) Effect of the transient expression (48 h) of procathepsin D (pCD), pCD D295N, pCD-KDEL (i.e. pCD fused to an endoplasmic reticulum retention signal) or glycopepsinogen (gPeps) on N1E-115 morphology. (E) Addition of conditioned medium collected from HeLa cells transfected with pCD, pCD D295N or gPeps for 24 h and followed by analysis of cellular morphology. The graphs in B–E represent the percentage (mean±s.d.) of N1E-115 cells exhibiting 'type 2' morphology (A) calculated from a minimum of five independent experiments (see Materials and Methods for details on counting). **P*<0.05, ***P*<0.01, ****P*<0.001 (one-way ANOVA followed by Bonferroni's multiple comparison tests in B, D and E; two-tailed *t*-test was conducted in C).

prevent it, remain unclear but might involve protein kinase C (PKC). The phosphorylation of PKCα is decreased in triple *Sez6*, *Sez6l2* and *Sez6l2* knockout mice (Miyazaki et al., 2006) and several findings support a role for PKC activity in the regulation of neuronal differentiation (Larsson, 2006). For example, it has been reported that the activation of PKC in SH-SY-5Y neuroblastoma cells inhibits neurite outgrowth induced by serum deprivation or calpain inhibition (Shea et al., 1995), whereas PKC inhibition in Neuro2-a cells induces their differentiation (Miñana et al., 1990).

In conclusion, our results point out a cross-road between a newly identified endolysosomal trafficking route for cathepsin D and neuronal differentiation. This finding, coupled with neuron-specific expression of SEZ6L2 (Miyazaki et al., 2006), and with the reported observation that cathepsin D binding to LRP1 in fibroblasts promotes their outgrowth (Beaujouin et al., 2010), suggest a cell type specificity of some alternatives to the Man-6-P transport pathways and linkage of these pathways to specific cellular processes.

MATERIALS AND METHODS

Materials

Unless otherwise specified, chemicals were obtained from Sigma-Aldrich. The following antibodies were used: mouse anti-MYC (9B11, Cell Signaling), -FLAG (M2, Sigma-Aldrich), -GAPDH (71.1, Sigma), AP-1 (100/3, Sigma) and -AP-2 (100/2, Sigma), sheep anti-SEZ6L2 (AF4916, R&D Systems), goat anti-cathepsin D (R-20, Santa Cruz Biotechnology,

Journal of Cell Science (2016) 129, 557-568 doi:10.1242/jcs.179374

used for western blotting), rabbit anti-cytochrome c (H-104, Santa Cruz Biotechnology), rabbit anti-Vps26 (EPR13456, Abcam), mouse anti-LAMP-2 (H4B4, DSHB), horseradish peroxidase (HRP)-coupled and Alexa-Fluor-coupled secondary antibodies (DAKO and Life Technologies, respectively). Rabbit anti-cathepsin D (used for immunofluorescence and immunoprecipitations) and anti-CI-MPR antibodies were provided by Stuart Kornfeld (Washington University, St Louis, MO), and mouse anti-Sec61β antibody was from Bernhard Dobberstein's group (ZMBH, Heidelberg).

DNA constructs

pCMV6-*Sez6l2*-MYC-FLAG was obtained from Origene (Rockville, clone MR211200, NM_144926). Wild-type and mutant SEZ6L2–MYC–FLAG were prepared in pcDNA3.1 (+) using classical molecular biology techniques. pcDNA3.1-procathepsin D-MYC and glycopepsinogen–MYC were generously provided by Wang S. Lee (Washington University, St Louis, MO). A linker sequence coding for MYC and the ER retention signal KDEL was inserted at the Xho site located at the C-terminal of cathepsin D. The D295N mutation was introduced by the InFusion™ method (Clontech). pGEX-5X3 was used to generate GST fusion proteins with the C-terminal tail of SEZ6L2.

Affinity chromatography

Cathepsin D and pepsinogen affinity columns (~1 mg/ml sepharose 4B) were prepared by Walter Gregory (Washington University, St Louis, MO) using porcine spleen cathepsin D and porcine stomach pepsinogen. Bovine serum albumin (BSA) and acid α-glucosidase were coupled to CNBr-activated sepharose 4B (Sigma) following the manufacturer's instructions (~1 and ~6 mg/ml, respectively). A total of 10 mouse brains were homogenized in 10 ml of 0.25 M sucrose, 1 mM EDTA, 20 mM Hepes-NaOH, pH 7.2 and centrifuged for 55 min at 5000 ***g*** in a JA-20 rotor (4°C). All animal experiments were performed according to approved guidelines. The supernatant was filtered through cheesecloth, and the pellet was suspended in homogenization buffer and centrifuged for 40 min in the same conditions. The supernatant was pooled with the first one and centrifuged at 125,000 ***g*** in a 50Ti rotor for 1 h (4°C). The pellet was suspended in 20 mM Hepes-NaOH, pH 7.0, 1 mM EDTA, containing protease inhibitors (Roche), sonicated and incubated for 15 min on ice prior to centrifugation for 40 min at 125,000 ***g*** (50Ti rotor, 4°C). Next, proteins were extracted from pelleted membranes by incubation in ice-cold solubilization buffer [20 mM Mes-NaOH, pH 6.5, 0.1 M NaCl, 5 mM EDTA, 5% glycerol (w/v), 1% Triton X-100, and protease inhibitors] for 20 min on ice, followed by centrifugation at 100,000 ***g*** in a TLA100.3 rotor for 15 min (4°C). Approximately 1.2 mg proteins were loaded on 1-ml columns. The flow through was collected after 15 min at room temperature. The column was washed 7× with 1 ml of ice-cold solubilization buffer and bound proteins were eluted with ice-cold solubilization buffer +20 mM Na acetate (pH 4.5), solubilization buffer +1 M NaCl (pH 6.5) or 150 mM NaCl, 0.1 M glycine-NaOH, pH 3.5. The major protein bands that eluted at pH 4.5 were analyzed by mass spectrometry at the proteomic platform of Washington University in St. Louis (Fig. S1). Western blotting was performed on the collected fractions (adjusted to pH of 6.5–7.0), after trichloroacetic acid (TCA) precipitation to concentrate the proteins (i.e. washes and elution fractions).

Cell culture, transfection and counting

Raw264.7 (mouse macrophages), HeLa (human cervical carcinoma cells) and Hek293 (human embryonic kidney cells) (ATCC) were cultured in DMEM (LONZA) medium supplemented with 10% fetal bovine serum (FBS; Sigma), 100 units/ml penicillin and 100 µg/ml streptomycin (LONZA). The N1E-115 mouse neuroblastoma cell line was maintained in DMEM-F12 (Life Technologies) supplemented as described above. HeLa cells deficient for Ptase (stable *GNPTAB* knockout), were generated using the CRISPR–Cas9 technology, and were generously provided by Stuart Kornfeld. All cell lines were tested for mycoplasma contamination using the MycoAlert™ PLUS Mycoplasma Detection Kit (LONZA). Plasmids were transfected using X-tremeGENE9 (Roche). Silencing of *Sez6l2* in N1E-115 was achieved with ON-TARGETplus *Sez6l2* siRNAs (smartpool or individual siRNAs) and DharmaFECT 1 reagent (Dharmacon) following the manufacturer's instructions. The ON-TARGETplus non-targeting pool was used as a control. Transfection media were removed after 24 h, and observations conducted at 48 h post-transfection. Of note, the level of cathepsin D mRNA was measured in control and SEZ6L2-deficient cells by qRT-PCR, using FastStart Universal SYBR Green (Roche) and a 7300 Real-Time PCR System (Applied Biosystems). GAPDH was used as a housekeeping gene. To prepare conditioned medium, HeLa cells were transfected for 8 h (with a mock plasmid or *Sez6l2* constructs), then cultured for 48 h in DMEM-F12 (+FBS). After centrifugation for 5 min at 1000 ***g***, the medium was added on the N1E-115 cells for 24 h. In Figs 6 and 7, the ImageJ software (http://imagej.nih.gov/ij/) was used to count the number of N1E-115 cells exhibiting a round shape devoid of neurites, and the number of cells exhibiting a distended cytoplasm and neurite growth. A minimum of five phase-contrast pictures (randomly chosen fields) were taken per dish with a 10× objective, in a minimum of five independent experiments (minimum of 500 cells counted per experiment). Statistical significance was assessed using a two-tailed, Student's *t*-test, or one-way ANOVA followed by the Bonferroni's test for multiple comparisons.

Western blotting

Cell or mouse organ lysates (prepared in PBS with 1% Triton X-100 and protease inhibitors) and other samples were mixed with Laemmli's sample buffer (with DTT), heated for 5 min at 95°C, and resolved by SDS-PAGE. Proteins were transferred onto PVDF membranes (PerkinElmer) and detected using specific antibodies [diluted 1:1000, except for cathepsin D (1:250), and GAPDH (1:3000)], and HRP-coupled secondary antibodies (diluted 1:3000). The signals were revealed by chemiluminescence (Western Lightning® Plus–ECL, Perkin-Elmer). Signals were quantified with the ImageJ software and non-paired, two-tailed Student's *t*-tests were performed.

Preparation of CCVs from mouse brain

We used an adapted version of published centrifugation protocols (Blitz et al., 1977; Lindner, 2006). All experimental procedures were conducted in accordance with local regulations under the supervision of the Animal Ethics Committee of UNamur. Briefly, after homogenization of ten mouse brains (C57Bl/6, 3–6-month-old males) in homogenization buffer (100 mM Mes, pH 6.5, 0.5 mM $MgCl_2$, 1 mM EGTA, 0.02% NaN3 supplemented with protease inhibitors) by five passages in a Potter-elvehjem, the sample was centrifuged for 55 min at 5000 ***g*** in a JA-20 rotor, at 4°C. The supernatant was collected, and the pellet was suspended in homogenization buffer and re-centrifuged in the same conditions. The supernatants of these two centrifugations were pooled, cleared by passage through cheesecloth and centrifuged for 45 min at 125,000 ***g*** in a 50Ti rotor at 4°C. The pellet was suspended in homogenization buffer and re-centrifuged for 30 min in the same conditions, then suspended in ~2 volumes of homogenization buffer and subjected to three passages in the Potter-elvehjem. Next, one volume of this fraction was mixed with one volume of 12.5% Ficoll and 12.5% sucrose prepared in homogenization buffer and centrifuged for 40 min at 26,000 ***g*** in the 50Ti rotor, at 4°C. The supernatant was collected and mixed with three volumes of homogenization buffer prior to centrifugation for 40 min at 125,000 ***g*** in the same rotor. The CCV-containing pellet was then suspended in a small volume of homogenization buffer and homogenized by three passages in the Potter-elvehjem. Finally, it was loaded on top of a discontinuous sucrose gradient (40% at the bottom, then 30, 20, 10 and 5%), and centrifuged for 1 h at 88,000 ***g*** in a SW55Ti rotor at 4°C. 200 µl fractions were collected from the top of the tube and analyzed by western blotting. The fractions with the highest levels of the clathrin adaptor proteins AP-1 and AP-2 were pooled.

Morphological analyses

For immunofluorescence experiments, the cells were fixed with 4% paraformaldehyde in PBS for 10 min at room temperature. When indicated, the cells were permeabilized with PBS containing 0.5% saponin for 10 min. After blocking for 10 min at room temperature in

Journal of Cell Science

PBS containing BSA 1%, the cells were incubated with primary antibodies (1 h) and then Alexa-Fluor-coupled secondary antibodies (45 min) diluted in PBS containing 1% BSA (1:100 and 1:500 for primary and secondary antibodies, respectively). DAPI was used to label nuclei. Of note, for the detection of Vps26 and CI-MPR, the cells were fixed with 80% methanol and 20% acetone (pre-cooled at −80°C) for 20 min at −20°C, and incubated with PBS containing 0.05% saponin for 10 min at room temperature prior to blocking. The coverslip were mounted with Mowiol and signals were observed with a Leica confocal microscope.

For immunoelectron microscopy, HeLa cells transiently (48 h) transfected with SEZ6L2–MYC–FLAG were fixed by adding 4% (w/v) paraformaldehyde (PFA) in 0.1 M phosphate buffer (pH 7.4) to an equal volume of culture medium for 15 min at room temperature. Cells were post-fixed with 4% (w/v) PFA in 0.1 M phosphate buffer for 2 h at room temperature. Embedding, preparation of ultrathin cryosections and immunogold labeling was performed as previously described (Slot and Geuze, 2007) using 10-nm gold particles (Cell Microscopy Core, Utrecht, The Netherlands). Sections were analyzed in a Jeol 1200 EX electron microscope (Tokyo, Japan) at 80 kV.

Cell surface biotinylation assay

The cell surface levels of SEZ6L2 were measured by a cell surface biotinylation assay, as described previously (Boonen et al., 2008).

GST pulldown assay

GST proteins fused to the C-terminal tail of SEZ6L2 were expressed in *E. coli* BL21 (RIL) (Stratagene) and purified using glutathione–agarose (Sigma), following the manufacturer's instructions. 100 µg of purified GST fusion proteins were bound to 40 µl of glutathione–agarose at room temperature for 1 h. After two washes with PBS, the beads were incubated with HeLa cell lysates (prepared using PBS, pH 7.2, 0.5% Triton X-100 and 0.5% NP-40 and protease inhibitors) for 4 h at 4°C. After five washes, proteins were eluted with Laemmli's sample buffer (2×) containing fresh DTT, heated for 5 min at 95°C, and centrifuged for 1 min at 13,000 ***g***. The supernatant was used for western blotting.

Metabolic labeling

The cells were starved for 30 min in Met/Cys- and FBS-free medium, incubated with [^{35}S]Methionine/Cysteine (Met/Cys) (PerkinElmer) for 30 min in this medium (with FBS), washed, and incubated for an additional 4-h period in unlabeled complete medium. The protein of interest was immunoprecipitated and resolved by SDS-PAGE as described previously (Boonen et al., 2009). Signals were detected with a Cyclone™ Phosphor Imager, quantified with the OptiQuant™ software and the results were analyzed for statistical relevance using non-paired, two-tailed Student's *t*-tests.

Internalization assays

50 µg of anti-SEZ6L2 antibody were labeled with 0.5 mCi ^{125}iodine (I) using iodination tubes (Pierce), following the manufacturer's instructions. The cells were incubated with 500,000 cpm of ^{125}I-labeled antibody diluted in PBS containing 1% BSA for 30 min on ice. They were washed with ice-cold PBS, and incubated at 16°C for 0, 10, 20, 30, 60 or 90 min. Cell-surface-bound antibodies were removed by three washes with PBS followed by treatment with ice-cold trypsin in PBS (200 µg/ml) for 1 h on ice. The cells were lysed in 500 µl of 0.1 M NaOH, mixed with 4 ml of scintillation cocktail, and the internalized radioactivity was quantified with a Beckman Coulter LS6500+ counter.

Mouse procathepsin D (Sigma) was iodinated as described above. After three washes with PBS, the cells were incubated with 200,000–300,000 cpm/ml of pre-warmed culture medium (+FBS) for 30 min at 37°C. The cells were washed and incubated for 30 s with a solution of 0.5 M NaCl and 0.2 M acetic acid, pH 3.5 to remove cathepsin D proteins bound to the cell surface. The cells were lysed and counted.

Acknowledgements

We thank W. Gregory, Dr W. S. Lee and Dr S. Kornfeld (Washington University in St. Louis, MO, USA) for providing the cathepsin D and pepsinogen affinity columns, cathepsin D and glycopepsinogen cDNAs and Ptase-knockout cells. We are grateful to Dr E. van Meel (who was a PhD student in Dr Klumperman's laboratory at the time, UMC Utrecht, The Netherlands) for her help in the affinity purification of SEZ6L2. We also thank Dr Kornfeld, Dr van Meel (now at Leiden University, The Netherlands), and Dr A. Goffinet (UCL, Belgium) for their critical reading of the manuscript, as well as Tineke Veenendaal (UMC Utrecht) for her skilled technical contribution to electron microscopy analyses.

Competing interests

The authors declare no competing or financial interests.

Author contributions

M.B., J.K. and M.J. designed the experiments. M.B, C.S., F.G. and V.O. conducted the experiments. M.B. wrote the article. M.J. and J.K. reviewed and edited the article.

Funding

M.B. was a post-doctoral researcher of the Fonds de la Recherche Scientifique - FNRS (F.R.S.-FNRS, Belgium) at the time of the project. Part of this work was supported by the F.R.S.-FNRS [grant number CDR J.0055.13 to M.J.].

Supplementary information

Supplementary information available online at
http://jcs.biologists.org/lookup/suppl/doi:10.1242/jcs.179374/-/DC1

References

Authier, F., Mort, J. S., Bell, A. W., Posner, B. I. and Bergeron, J. J. (1995). Proteolysis of glucagon within hepatic endosomes by membrane-associated cathepsins B and D. *J. Biol. Chem.* **270**, 15798-15807.

Baranski, T. J., Faust, P. L. and Kornfeld, S. (1990). Generation of a lysosomal enzyme targeting signal in the secretory protein pepsinogen. *Cell* **63**, 281-291.

Beaujouin, M., Prébois, C., Derocq, D., Laurent-Matha, V., Masson, O., Pattingre, S., Coopman, P., Bettache, N., Grossfield, J., Hollingsworth, R. E. et al. (2010). Pro-cathepsin D interacts with the extracellular domain of the beta chain of LRP1 and promotes LRP1-dependent fibroblast outgrowth. *J. Cell Sci.* **123**, 3336-3346.

Blitz, A. L., Fine, R. E. and Toselli, P. A. (1977). Evidence that coated vesicles isolated from brain are calcium-sequestering organelles resembling sarcoplasmic reticulum. *J. Cell Biol.* **75**, 135-147.

Boonen, M., Rezende de Castro, R., Cuvelier, G., Hamer, I. and Jadot, M. (2008). A dileucine signal situated in the C-terminal tail of the lysosomal membrane protein p40 is responsible for its targeting to lysosomes. *Biochem. J.* **414**, 431-440.

Boonen, M., Vogel, P., Platt, K. A., Dahms, N. and Kornfeld, S. (2009). Mice lacking mannose 6-phosphate uncovering enzyme activity have a milder phenotype than mice deficient for N-acetylglucosamine-1-phosphotransferase activity. *Mol. Biol. Cell.* **20**, 4381-4389.

Boonen, M., van Meel, E., Oorschot, V., Klumperman, J. and Kornfeld, S. (2011). Vacuolization of mucolipidosis type II mouse exocrine gland cells represents accumulation of autolysosomes. *Mol. Biol. Cell* **22**, 1135-1147.

Braulke, T. and Bonifacino, J. S. (2009). Sorting of lysosomal proteins. *Biochim. Biophys. Acta* **1793**, 605-614.

Canuel, M., Korkidakis, A., Konnyu, K. and Morales, C. R. (2008). Sortilin mediates the lysosomal targeting of cathepsins D and H. *Biochem. Biophys. Res. Commun.* **373**, 292-297.

Cullen, V., Lindfors, M., Ng, J., Paetau, A., Swinton, E., Kolodzeij, P., Boston, H., Saftig, P., Woulfe, J., Feany, M. B. et al. (2009). Cathepsin D expression level affects alpha-synuclein processing, aggregation, and toxicity in vivo. *Mol. Brain.* **2**, 5.

Derocq, D., Prébois, C., Beaujouin, M., Laurent-Matha, V., Pattingre, S., Smith, G. K. and Liaudet-Coopman, E. (2012). Cathepsin D is partly endocytosed by the LRP1 receptor and inhibits LRP1-regulated intramembrane proteolysis. *Oncogene* **31**, 3202-3212.

Diment, S. and Stahl, P. (1985). Macrophage endosomes contain proteases which degrade endocytosed protein ligands. *J. Biol. Chem.* **260**, 15311-15317.

Dittmer, F., Ulbrich, E. J., Hafner, A., Schmahl, W., Meister, T., Pohlmann, R. and von Figura, K. (1999). Alternative mechanisms for trafficking of lysosomal enzymes in mannose 6-phosphate receptor-deficient mice are cell type-specific. *J. Cell Sci.* **112**, 1591-1597.

Ghosh, P., Dahms, N. M. and Kornfeld, S. (2003). Mannose 6-phosphate receptors: new twists in the tale. *Nat. Rev. Mol. Cell Biol.* **4**, 202-213.

Glickman, J. N. and Kornfeld, S. (1993). Mannose 6-phosphate-independent targeting of lysosomal enzymes in I-cell disease B lymphoblasts. *J. Cell Biol.* **123**, 99-108.

Gunnersen, J. M., Kim, M. H., Fuller, S. J., De Silva, M., Britto, J. M., Hammond, V. E., Davies, P. J., Petrou, S., Faber, E. S. L., Sah, P. et al. (2007). Sez-6 proteins affect dendritic arborization patterns and excitability of cortical pyramidal neurons. *Neuron* **56**, 621-639.

Hamer, I. and Jadot, M. (2005). Endolysosomal transport of newly-synthesized cathepsin D in a sucrose model of lysosomal storage. *Exp. Cell Res.* **309**, 284-295.
Koch, S., Molchanova, S. M., Wright, A. K., Edwards, A., Cooper, J. D., Taira, T., Gillingwater, T. H. and Tyynelä, J. (2011). Morphologic and functional correlates of synaptic pathology in the cathepsin D knockout mouse model of congenital neuronal ceroid lipofuscinosis. *J. Neuropathol. Exp. Neurol.* **70**, 1089-1096.
Koch, S., Scifo, E., Rokka, A., Trippner, P., Lindfors, M., Korhonen, R., Corthals, G. L., Virtanen, I., Lalowski, M. and Tyynelä, J. (2013). Cathepsin D deficiency induces cytoskeletal changes and affects cell migration pathways in the brain. *Neurobiol. Dis.* **50**, 107-119.
Koike, M., Nakanishi, H., Saftig, P., Ezaki, J., Isahara, K., Ohsawa, Y., Schulz-Schaeffer, W., Watanabe, T., Waguri, S., Kametaka, S. et al. (2000). Cathepsin D deficiency induces lysosomal storage with ceroid lipofuscin in mouse CNS neurons. *J. Neurosci.* **20**, 6898-6906.
Kollmann, K., Damme, M., Markmann, S., Morelle, W., Schweizer, M., Hermans-Borgmeyer, I., Röchert, A. K., Pohl, S., Lübke, T., Michalski, J.-C. et al. (2012). Lysosomal dysfunction causes neurodegeneration in mucolipidosis II 'knock-in' mice. *Brain* **135**, 2661-2675.
Konyukh, M., Delorme, R., Chaste, P., Leblond, C., Lemière, N., Nygren, G., Anckarsäter, H., Rastam, M., Ståhlberg, O., Amsellem, F. et al. (2011). Variations of the candidate SEZ6L2 gene on Chromosome 16p11.2 in patients with autism spectrum disorders and in human populations. *PLoS ONE* **6**, e17289.
Kornfeld, S. and Sly, W. S. (2000). I-cell disease and pseudo-Hurler polydystrophy: disorders of lysosomal enzyme phosphorylation and localization. In *The Metabolic and Molecular Bases of Inherited Disease* (ed. C. R. Schriver, A. L. Baudet, W. S. Sly and D. Valle), pp. 3469-3483. New York: McGraw-Hill.
Kuhn, P.-H., Koroniak, K., Hogl, S., Colombo, A., Zeitschel, U., Willem, M., Volbracht, C., Schepers, U., Imhof, A., Hoffmeister, A. et al. (2012). Secretome protein enrichment identifies physiological BACE1 protease substrates in neurons. *EMBO J.* **31**, 3157-3168.
Kumar, R. A., Marshall, C. R., Badner, J. A., Babatz, T. D., Mukamel, Z., Aldinger, K. A., Sudi, J., Brune, C. W., Goh, G., Karamohamed, S. et al. (2009). Association and mutation analyses of 16p11.2 autism candidate genes. *PLoS ONE* **4**, e4582.
Larsson, C. (2006). Protein kinase C and the regulation of the actin cytoskeleton. *Cell Signal.* **18**, 276-284.
Laurent-Matha, V., Derocq, D., Prébois, C., Katunuma, N. and Liaudet-Coopman, E. (2006). Processing of human cathepsin D is independent of its catalytic function and auto-activation: involvement of cathepsins L and B. *J. Biochem.* **139**, 363-371.
Lefrancois, S., Zeng, J., Hassan, A. J., Canuel, M. and Morales, C. R. (2003). The lysosomal trafficking of sphingolipid activator proteins (SAPs) is mediated by sortilin. *EMBO J.* **22**, 6430-6437.
Lindner, R. (2006). Purification of clathrin-coated vesicles from bovine brain, liver, and adrenal gland. In *Cell Biology, A Laboratory Handbook*, 3rd edn (ed. J. E. Celis), pp. 51-56. Amsterdam, Netherlands: Elsevier.
Ludwig, T., Munier-Lehmann, H., Bauer, U., Hollinshead, M., Ovitt, C., Lobel, P. and Hoflack, B. (1994). Differential sorting of lysosomal enzymes in mannose 6-phosphate receptor-deficient fibroblasts. *EMBO J.* **13**, 3430-3437.
Markmann, S., Thelen, M., Cornils, K., Schweizer, M., Brocke-Ahmadinejad, N., Willnow, T., Heeren, J., Gieselmann, V., Braulke, T. and Kollmann, K. (2015). Lrp1/LDL receptor play critical roles in mannose 6-phosphate-independent lysosomal enzyme targeting. *Traffic* **16**, 743-759.
Miñana, M. D., Felipo, V. and Grisolía, S. (1990). Inhibition of protein kinase C induces differentiation in Neuro-2a cells. *Proc. Natl. Acad. Sci. USA* **87**, 4335-4339.
Miyazaki, T., Hashimoto, K., Uda, A., Sakagami, H., Nakamura, Y., Saito, S.-Y., Nishi, M., Kume, H., Tohgo, A., Kaneko, I. et al. (2006). Disturbance of cerebellar synaptic maturation in mutant mice lacking BSRPs, a novel brain-specific receptor-like protein family. *FEBS Lett.* **580**, 4057-4064.
Mulley, J. C., Iona, X., Hodgson, B., Heron, S. E., Berkovic, S. F., Scheffer, I. E. and Dibbens, L. M. (2011). The role of seizure-related SEZ6 as a susceptibility gene in febrile seizures. *Neurol. Res. Int.* **2011**, 917565.
Pohl, S., Tiede, S., Marschner, K., Encarnação, M., Castrichini, M., Kollmann, K., Muschol, N., Ullrich, K., Müller-Loennies, S. and Braulke, T. (2010). Proteolytic processing of the gamma-subunit is associated with the failure to form GlcNAc-1-phosphotransferase complexes and mannose 6-phosphate residues on lysosomal enzymes in human macrophages. *J. Biol. Chem.* **285**, 23936-23944.
Pohlmann, R., Boeker, M. W. C. and von Figura, K. (1995). The two mannose 6-phosphate receptors transport distinct complements of lysosomal proteins. *J. Biol. Chem.* **270**, 27311-27318.
Reczek, D., Schwake, M., Schröder, J., Hughes, H., Blanz, J., Jin, X., Brondyk, W., Van Patten, S., Edmunds, T. and Saftig, P. (2007). LIMP-2 is a receptor for lysosomal mannose-6-phosphate-independent targeting of beta-glucocerebrosidase. *Cell* **131**, 770-783.
Rijnboutt, S., Kal, A. J., Geuze, H. J., Aerts, H. and Strous, G. J. (1991). Mannose 6-phosphate-independent targeting of cathepsin D to lysosomes in HepG2 cells. *J. Biol. Chem.* **266**, 23586-23592.
Rijnboutt, S., Stoorvogel, W., Geuze, H. J. and Strous, G. J. (1992). Identification of subcellular compartments involved in biosynthetic processing of cathepsin D. *J. Biol. Chem.* **267**, 15665-15672.
Sardiello, M., Palmieri, M., di Ronza, A., Medina, D. L., Valenza, M., Gennarino, V. A., Di Malta, C., Donaudy, F., Embrione, V., Polishchuk, R. S. et al. (2009). A gene network regulating lysosomal biogenesis and function. *Science* **24**, 473-477.
Sevlever, D., Jiang, P. and Yen, S.-H. C. (2008). Cathepsin D is the main lysosomal enzyme involved in the degradation of alpha-synuclein and generation of its carboxy-terminally truncated species. *Biochemistry* **47**, 9678-9687.
Shea, T. B., Cressman, C. M., Spencer, M. J., Beermann, M. L. and Nixon, R. A. (1995). Enhancement of neurite outgrowth following calpain inhibition is mediated by protein kinase C. *J. Neurochem.* **65**, 517-527.
Siintola, E., Partanen, S., Stromme, P., Haapanen, A., Haltia, M., Maehlen, J., Lehesjoki, A.-E. and Tyynela, J. (2006). Cathepsin D deficiency underlies congenital human neuronal ceroid-lipofuscinosis. *Brain* **129**, 1438-1445.
Slot, J. W. and Geuze, H. J. (2007). Cryosectioning and immunolabeling. *Nat. Protoc.* **2**, 2480-2491.
Steinfeld, R., Reinhardt, K., Schreiber, K., Hillebrand, M., Kraetzner, R., Bruck, W., Saftig, P. and Gartner, J. (2006). Cathepsin D deficiency is associated with a human neurodegenerative disorder. *Am. J. Hum. Genet.* **78**, 988-998.
Stützer, I., Selevsek, N., Esterházy, D., Schmidt, A., Aebersold, R. and Stoffel, M. (2013). Systematic proteomic analysis identifies β-site amyloid precursor protein cleaving enzyme 2 and 1 (BACE2 and BACE1) substrates in pancreatic β-cells. *J. Biol. Chem.* **288**, 10536-10547.
Tyynelä, J., Sohar, I., Sleat, D. E., Gin, R. M., Donnelly, R. J., Baumann, M., Haltia, M. and Lobel, P. (2000). A mutation in the ovine cathepsin D gene causes a congenital lysosomal storage disease with profound neurodegeneration. *EMBO J.* **19**, 2786-2792.
van Meel, E., Boonen, M., Zhao, H., Oorschot, V., Ross, F. P., Kornfeld, S. and Klumperman, J. (2011). Disruption of the Man-6-P targeting pathway in mice impairs osteoclast secretory lysosome biogenesis. *Traffic* **12**, 912-924.
Wähe, A., Kasmapour, B., Schmaderer, C., Liebl, D., Sandhoff, K., Nykjaer, A., Griffiths, G. and Gutierrez, M. G. (2010). Golgi-to-phagosome transport of acid sphingomyelinase and prosaposin is mediated by sortilin. *J. Cell Sci.* **123**, 2502-2511.
Xu, C., Mullersman, J. E., Wang, L., Bin Su, B., Mao, C., Posada, Y., Camarillo, C., Mao, Y., Escamilla, M. A. and Wang, K.-S. (2013). Polymorphisms in seizure 6-like gene are associated with bipolar disorder I: evidence of gene×gender interaction. *J. Affect. Disord.* **145**, 95-99.
Yaguchi, H., Yabe, I., Takahashi, H., Okumura, F., Takeuchi, A., Horiuchi, K., Kano, T., Kanda, A., Saito, W., Matsumoto, M. et al. (2014). Identification of anti-SEZ6L2 antibody in a patient with cerebellar ataxia and retinopathy. *J. Neurol.* **261**, 224-226.
Yu, Z.-L., Jiang, J.-M., Wu, D.-H., Xie, H.-J., Jiang, J.-J., Zhou, L., Peng, L. and Bao, G.-S. (2007). Febrile seizures are associated with mutation of seizure-related (SEZ) 6, a brain-specific gene. *J. Neurosci. Res.* **85**, 166-172.

Journal of Cell Science